# TRAVELING WAVE SYNCHRONOUS ELECTROHYDRODYNAMIC POWER GENERATION

by
WILLIAM F. REEVE
THESIS SUPERVISOR:
PROFESSOR J. R. MELCHER

SUBMITTED: May 19, 1967

# TRAVELING WAVE SYNCHRONOUS ELECTROHYDRODYNAMIC POWER GENERATION

by

WILLIAM F. REEVE II

BSEE UNIVERSITY OF NOTRE DAME

(1957)

SUBMITTED TO THE DEPARTMENT OF NAVAL ARCHITECTURE AND MARINE ENGINEERING IN PARTIAL FULFILLMENT OF THE REQUIREMENTS OF THE MASTER OF SCIENCE DEGREE IN ELECTRICAL ENGINEERING AND THE PROFESSIONAL DEGREE, NAVAL ENGINEER

at the

MASSACHUSETTS INSTITUTE OF TECHNOLOGY

May, 1967

Signature of Author . . . . . .
Department of Naval Architecture and Marine Engineering, May 19, 1967.

Certified by . . . . . .
Thesis Supervisor

Certified by . . . . . .
Reader for the Department

Accepted by . . . . . .
Chairman, Departmental Committee on Graduate Students

# TRAVELING WAVE SYNCHRONOUS ELECTROHYDRODYNAMIC POWER GENERATION

by

WILLIAM F. REEVE

## ABSTRACT

Submitted to the Department of Naval Architecture and Marine Engineering on May 19, 1967 in partial fulfillment of the requirements for the Master of Science Degree in Electrical Engineering and the Professional Degree, Naval Engineer.

Electrohydrodynamic power generation has become a field of intense interest during the past few years. The utilization of electric fields for power generation does permit the use of a lighter generator structure which is relatively free of moving parts. To date, most of the efforts in this field have been devoted to DC power generation. AC power generation is also possible if traveling wave synchronous interactions, similar to those employed in the conventional synchronous generator, are used.

An examination of the field equations of the EHD generator demonstrates that the expressions for the developed power closely parallel those of the conventional synchronous machine. Consideration of the long wavelength limit shows that the power expressions can be manipulated in such a fashion as to infer an equivalent circuit model of the EHD generator which is the exact dual of the cylindrical rotor synchronous generator equivalent circuit.

A prototype EHD generator was built to demonstrate the qualitative aspects of the device and to compare the performance of the generator with that predicted by the equivalent circuit model.

Reasonable agreement with the model predictions was achieved. The prototype demonstrated many of the associated problems which must be overcome before the device can be optimized. Careful design considerations can eliminate or reduce these problems appreciably. The AC traveling wave synchronous generator shows promise of being able to compete with the DC EHD generator in a relatively short period of time.

Thesis Supervisor: James R. Melcher
Title: Associate Professor of Electrical Engineering

TABLE OF CONTENTS

## ACKNOWLEDGEMENTS

The author wishes to express his appreciation to Professor James R. Melcher, Department of Electrical Engineering, Massachusetts Institute of Technology for providing the topic of this project and his continued interest and guidance in developing a sound approach to the problem; to Lance Herold whose contemporary thesis provided the means by which suitable charged particle distributions were developed for studying the generator behavior; to Harold Atlas for his help and beneficial suggestions; to Mrs. James Glynn for typing the final report; and to my wife, Victoria, for her encouragement and help during these past three years.

This project was supported by funds provided by the National Aeronautics and Space Administration, and the United States Navy, whose financial aid is gratefully acknowledged.

# LIST OF SYMBOLS

$P_m$ . . . . . Developed Electromagnetic Power

$\omega$ . . . . . Angular frequency (radians per second)

$F_r$ . . . . . Rotor MMF wave

$F_s$ . . . . . Stator MMF wave

$\theta, \delta$ . . . . . Phase angles

$U$ . . . . . Stream velocity

$f$ . . . . . Frequency (cycles per second)

$\lambda$ . . . . . Wavelength

$k$ . . . . . Wave number

$\phi$ . . . . . Electric field potential

$\sigma$ . . . . . Surface charge

$P_d$ . . . . . Developed Electrohydrodynamic power

$\epsilon_o$ . . . . . Permittivity of free space

$a, b, c, d$ . . . . . Linear dimensions

$P_l$ . . . . . Power delivered to a resistive load

$G$ . . . . . Conductance (mhos)

$R$ . . . . . Resistance (ohms)

$C$ . . . . . Capacitance (farads)

$R_\ell$ . . . . . Load Resistance

$i_o$ . . . . . Current source current level

$\bar{i}_o$ . . . . . Average current from current sources

$i_r$ . . . . . Load current

$\mu$ . . . . . Micro ($10^{-6}$)

M . . . . . Meg ($10^6$)

$\hat{N}$ . . . . . Complex number N

$\hat{N}^*$ . . . . . Complex conjugate of N

$X_c$ . . . . . Capacitive reactance

$\nabla$ . . . . . Operator "del"

E . . . . . Electric field

$\tau$ . . . . . Stress tensor

$\eta$ . . . . . Efficiency

A . . . . . Lateral area

$v_p$ . . . . . Particle velocity

j . . . . . $\sqrt{-1}$

$R_e$ . . . . . "Real part of"

$\langle\ \rangle$ . . . . . Time average

# INTRODUCTION

Little attention has been focused in the past on the utilization of electric fields for power generation applications. It has long been realized that the power densities which can be generated by means of electric fields do not compare favorably with those which can be achieved by utilizing magnetic field interactions. Large magnetic field densities can be achieved through the use of ferromagnetic materials but this implies that the generator must inherently possess a high density factor. Weight was never a major problem in the past. However, the space age has now imposed the possibility of a major weight problem, and the means by which power may be generated through electrohydrodynamic coupling has become a significant area of investigation. The major limitations on such devices is the electrical breakdown strength of the environment in which they are functioning, and the amount of charge which may be deposited on the fluid.

## Magnetic AC Synchronous Interaction

The majority of standard AC power generating is accomplished through ferromagnetic synchronous 3 phase generators. These machines utilize the interaction of two sinusoidal magnetic fields rotating in space at a synchronous speed. One of the fields, the rotor field, is obtained by applying a DC voltage to the rotor of the machine through slip rings. The sinusoidal distribution is achieved by the winding connection on the rotor. When the rotor is turned by means of a prime mover, the magnetic

field becomes a sinusoidal rotating (traveling) wave in space. The rotating stator magnetic field is also achieved by winding considerations. The windings on the stator are distributed about the inner periphery and are spacially phased at an angle of $\frac{360}{n}$ electrical degrees apart where n represents the total phases in the stator winding. As the rotor sweeps past the windings, a sinusoidal standing wave voltage is induced in each of the phases. This voltage gives rise to a sinusoidal magnetic field in each phase, whose amplitude is dependent upon the load demands placed on the generator. The resultant wave of the n-phased standing magnetic fields is a rotating sinusoidal magnetic field. Thus, the rotor and the stator fields both rotate in space at the same synchronous speed although they are spacially separated by an angle $\Theta$. (This angle will change whenever the magnitude of either the rotor field or stator field is changed.)

The expression for the electromechanical power developed by such a device can be simplified to the following form:

$$P_m = K_m \omega F_r F_s \sin \Theta \qquad (1)$$

where, $\omega$ is the synchronous angular frequency

$F_r$ is the magnitude of the rotor MMF wave.

$F_s$ is the magnitude of the stator MMF wave.

$K_m$ is a constant reflecting dimensional factors of the generator and the permeability of the air gap.

$\Theta$ is the spacial phase angle by which the rotor field and stator field are separated.

## EHD Synchronous Interactions

Turning our attention to EHD synchronous machines, it can easily be demonstrated that marked similarities do exist between the behavioral characteristics of the EHD machine and the magnetic AC synchronous machine. Consider a linear synchronous machine of the basic form shown in Figure 1.

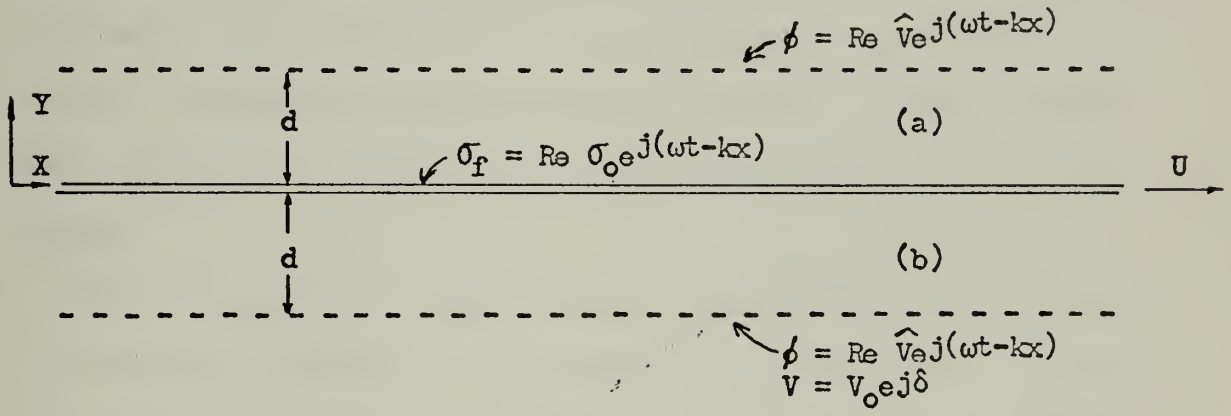


Figure 1: A Linear Synchronous AC Machine.

A very thin stream of charged particles, whose width extends into the paper, moving with a velocity U is introduced into a chamber. The stream of particles may be described as $\sigma_f = Re\ \sigma_o\ \epsilon^{j(\omega t-kx)}$, where k is the wave number and is equal to $\frac{2\pi}{\lambda}$. $\lambda$ is the wavelength. $\sigma_o$ is the magnitude of the maximum surface charge. The relationship between k, $\omega$, and U is as follows:

$$U = f\lambda = \frac{\omega}{2\pi}\lambda = \frac{\omega}{k} \qquad (2)$$

The walls of the chamber have a sinusoidal traveling voltage wave

impressed on them which has the form $V = Re\ \hat{V}\ \epsilon^{j(\omega t - kx)}$. The voltage wave is moving down the channel with the same velocity as the stream of charged particles. The time dependence of both sinusoidal distributions is the same, thus the voltage wave and the stream of charged particles are locked in synchronism as they move down the channel. The complex voltage $\hat{V} = V_o\ \epsilon^{j\delta}$ where $\delta$ is the spatial phase angle between the particle stream and the impressed traveling voltage. Traveling voltage waves may be approximated by electrodes, suitably spaced, which have n-phased and properly sequenced voltages impressed on them. The EHD machine channel is perfectly symmetrical with respect to the particle stream.

The solution to the field problem suggested by this configuration is developed in Appendix A I. The final result shows that the electro-hydrodynamic power developed capable of being converted to electrical energy is:

$$P_d' = K_e' \omega V_o \sigma_o \sin \delta$$

This equation may be modified to the following form by simply changing the constant term of the equation:

$$P_d' = K_e \omega \frac{V_o}{d} \frac{\sigma_o}{2\epsilon_o} \sin \delta \qquad (3)$$

where $\frac{V_o}{d}$ represents the order of magnitude of the maximum field intensity which can be anticipated in the channel if the voltage wave alone were present, $(E_v)$, and $\frac{\sigma_o}{2\epsilon_o}$ is the maximum field intensity

just above or below the stream of charged particles due to the presence of the charge alone ($E_\sigma$).

Thus equation (3) may be rewritten in the following form:

$$P_d' = K_e \omega E_v E_\sigma \sin \delta$$

where $\omega$ is again the synchronous angular frequency and $K_e$ is a constant reflecting the dimensional factors of the generator and the permittivity of free space.

Equations (1) and (4) are identical in format. Thus the electric and magnetic field synchronous interactions suggest that a possible dualism exists in these mechanisms.

## Generator Behavior in the Presence of a Continuous Resistive Loading

The next step in the analysis of an EHD synchronous generator is to consider pure generator action. This entails the introduction of the stream of charged particles, but the traveling voltage wave is induced on the electrodes by the charge. This is analagous to inducing a voltage in the stator windings of the standard synchronous machine through electromagnetic coupling. The loading of the generator will be accomplished by connecting a continuous resistive load to the generator channel. The load is connected to a ground plane which is held at a zero potential. The load is described by a linear conductance of G mhos per meter in the X direction. Figure 2 shows a diagramatic model of the generator in the loaded condition.

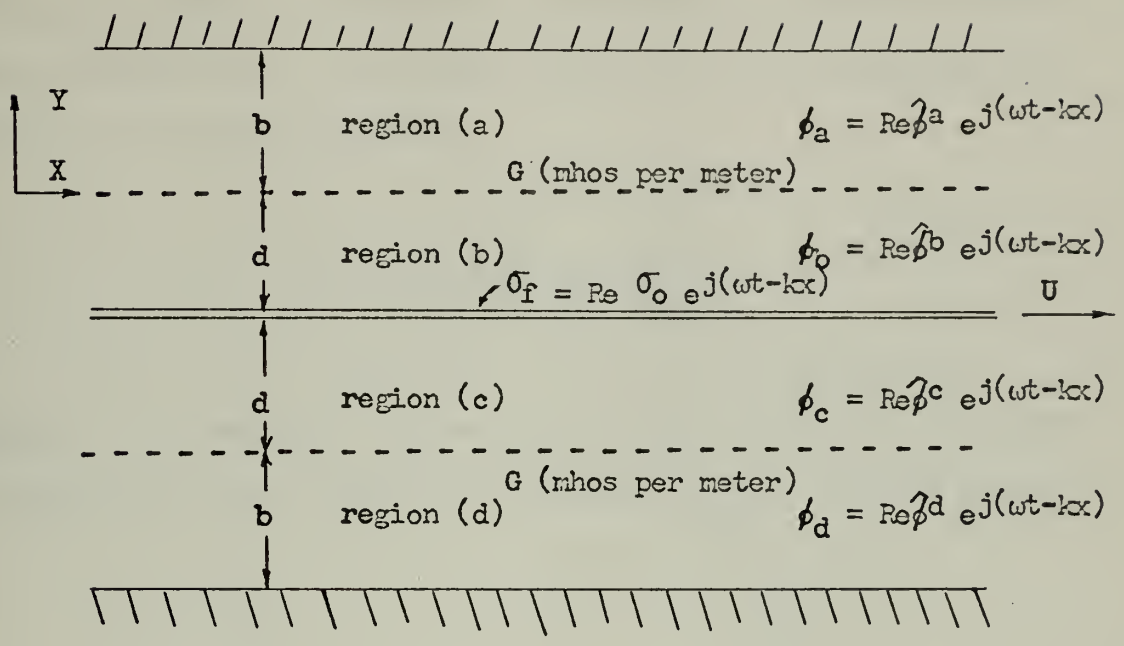


Figure 2: Top View of a Continuously Loaded AC EHD Synchronous Generator

The field equations of this model are developed in Appendix A II. The final expression for the time average power per unit length delivered to the load is:

$$\langle P_1 \rangle = \frac{\frac{G}{2}\left[\frac{\sigma_o \sinh kb}{2\epsilon_o k}\right]^2}{\cosh^2 k(b+d) + \left(\frac{G}{\omega a \epsilon_o k}\right)^2 \sinh kb^2 \cosh^2 kd}$$

Although the equation appears quite complicated, consideration of the long wavelength limit which implies that $\lambda >> b$ or d, simplifies the equation to the following form:

$$\langle P_1 \rangle = \frac{G (\sigma_o \omega a b)^2}{8 \left[\omega^2 a^2 \epsilon_o^2 + G^2 b^2\right]}$$

Appendix A III rearranges this equation in such a manner as to suggest an equivalent circuit model for the machine which is shown in Figure 3.

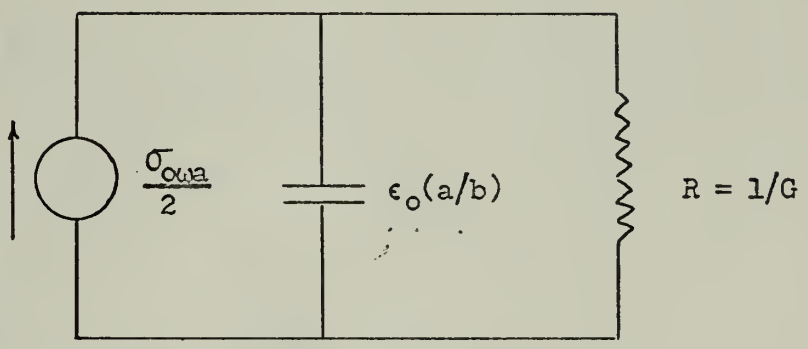


Figure 3: The Proposed Equivalent Circuit Model for the EHD Synchronous Generator. All quantities are for a per unit length basis.

The equivalent circuit applies on a per unit length basis. If the unit length selected is that of the electrode width, then the circuit represents an equivalent circuit model for each pair of electrodes. This circuit verifies the dualistic behavior of the two types of

synchronous machines, since the equivalent circuit of the synchronous ferromagnetic generator is a voltage source in series with an inductive reactance and a load impedance.

Maximum power transfer in such a circuit is achieved when the resistance is equal to the shunt capacitive reactance. A graphical representation of power delivered to the load as a function of load resistance is shown in Figure 4. If the load resistances can be achieved, the curve can be the basis for checking the validity of the model.

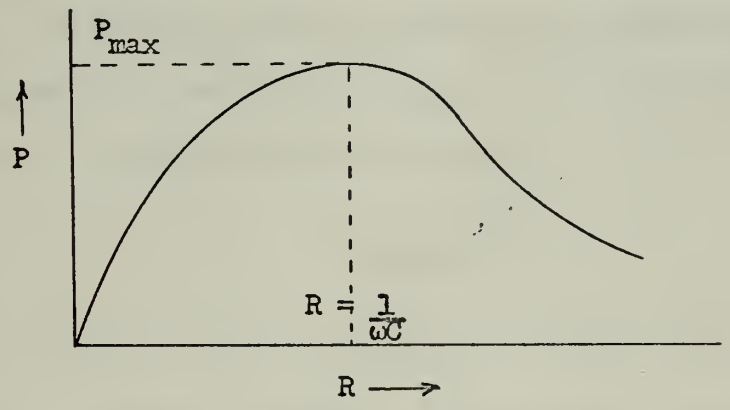


Figure 4: The variation of power delivered to the load as a function of load resistance for the proposed circuit model.

Although the entire development of the electrohydrodynamic synchronous interaction principles is based on a continuum medium, the utilization of discrete electrodes does permit the continuum to be approached experimentally.

## DESCRIPTION AND DESIGN HISTORY OF THE GENERATOR

The generator was primarily a wind tunnel type of structure. The main air stream velocity (U) was provided by a 250 CFM axial flow fan with a three phase induction motor drive. The air velocity was controlled by a three phase rheostat in the supply line which governed the slip of the induction motor. A diffuser section of plexiglass and wood concentrated the air stream before entering the main generator section. An aluminum flow straightener was mounted in the diffuser. The two remaining sections, the exciter and the electrode chamber, were the primary components of the generator.

### The Exciter

The exciter[1] provided the stream of charged particles for the generator. The first attempts to investigate a possible exciter used a fine tubing mechanism which released particles under a pressure head into the air stream. These particles were subjected of a charging potential of 2000 to 4000 peak volts at a 60 cycle per second frequency.

---

[1] The design of the exciter section is the product of a concurrent thesis. For a more elaborate discussion of the exciter see TRAVELING WAVE CHARGED PARTICLE GENERATION, L. HEROID, SM Thesis, Massachusetts Institute of Technology (1967).

(Sixty cycles per second were used throughout the experiment.) The output signal was very random, primarily due to the fact that the release of particles in this manner was itself random. Multiple tubes were then used, but much of the same effect was noted. Next, commercial spray nozzles were tried. These nozzles released a spray of very fine particles. An annular electrode was mounted near the nozzle throat, and with a charging potential of only 50 volts RMS, a relatively pure sinusoidal output was achieved. Peak signal strength was increased by two orders of magnitude due to the increase in charge transporting capability which is functionally related to the concentrated field strength and the increase in particle density. Random signals were no longer encountered. The commercial nozzles suffered from the fact that they had to be mounted perpendicular to the air flow and a majority of the particles simply sprayed on the opposite sides of the electrode chamber. A large percentage of the charged particles were lost before they effectively interacted with any of the electrodes.

The commercial spray nozzles, however, determined the subsequent design patterns which followed. It was evident that small particles in copious quantities were necessary, and that reduced charging voltages could accomplish the desired effect easily if proper field strengths were used. A series of spray nozzles was then designed which introduced fine particles directly into the air stream from thin elements mounted vertically in the air flow. The final designs used an ejector principle to introduce the particles into the air stream.

Perpendicular water headers were mounted on the exciter walls. Thin tubular connections led from the header to the verticle elements. Compressed air was introduced at the top and bottom of a circular section drilled through the center of the vertical element. The air was released through small nozzle outlets mounted in the downstream face of the vertical elements. The exhausting air created a vacuum in the header and the water was drawn up into the header from a water resevoir and forced out through the nozzle openings. The electrode for charging the particles was painted on the downstream face of the vertical element with a silver conducting paint. The upstream face was ellipsoidal in shape to reduce air turbulence, while the downstream face was a blunt flat surface. The water connection was used for a ground point. A charging potential of 200 volts RMS produced an increase in peak signal strength of two more orders of magnitude. A net overall improvement of five orders of magnitude in the ratio of peak output current level to charging potential was achieved in reaching the final design. Figure 5 shows the exciter section which was used in making the load measurements on the generator. Another exciter section releasing particles under air pressure is shown in Figure 6.

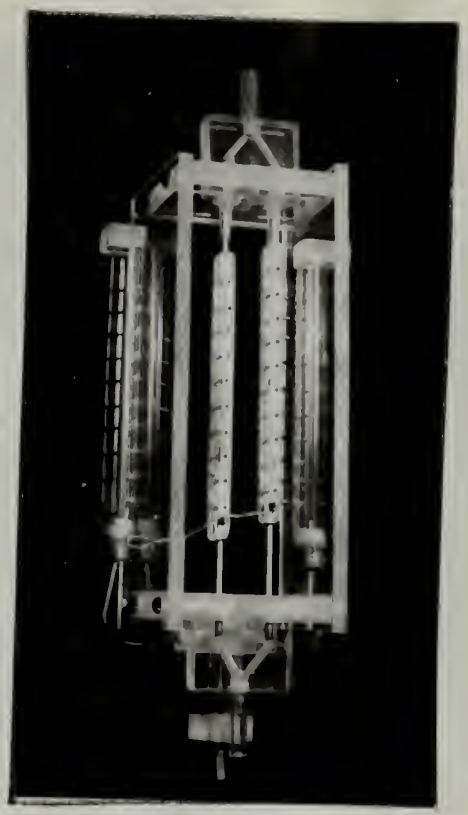

Figure 5: The exciter section used for measuring the generator performance. Note the vertical headers and the connections to the vertical elements. The nozzles are mounted in the face.

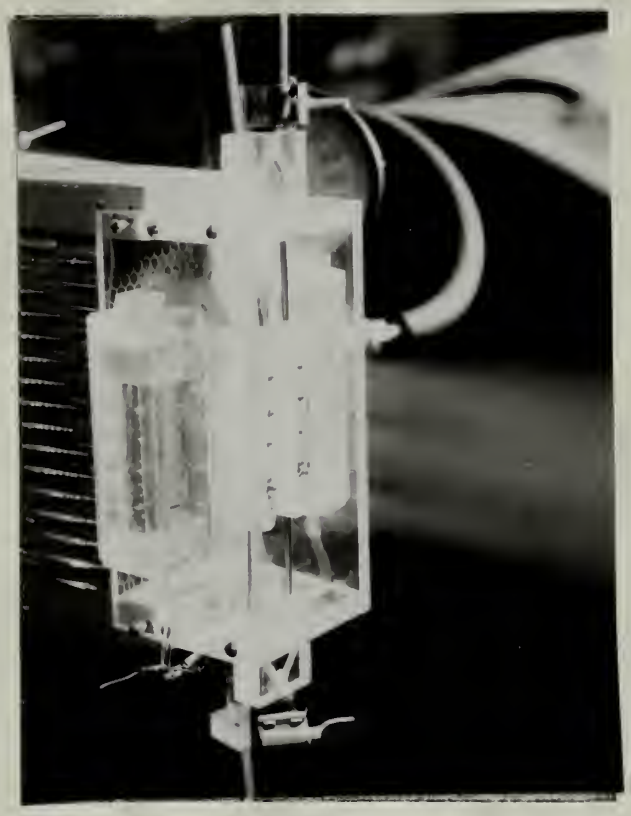

Figure 6: An exciter section delivering a stream of water particles.

## The Electrode Chamber

The exciter section married directly to the electrode chamber. The electrodes were painted on the interior of the channel with a conducting paint. There were eighteen pairs of electrodes in all. The electrodes had similar dimensions, one inch in width and four inches in height. Connections led from the electrodes to the exterior load resistors. In addition, one megohm resistors are connected in series with the load resistances for current measurement purposes. Resistance levels in EHD applications are so high that one megohm approaches short circuit conditions.

The electrodes, in addition to being one inch wide, were spaced one inch apart. These distances were selected so that the interaction of the particle stream and the traveling wave could be studied using impressed high voltages from a six phase transformer. These distances would allow a peak potential difference of 30KV between electrodes before breakdown would occur. However, this latter group of experiments was abandoned because it would add little additional insight, and was relatively difficult in comparison to the pure generator studies.

The channel was constructed of 3/8 inch plexiglass and was 36 inches in length, 2-1/4 inches in width, and had an overall height of 6-1/4 inches. These dimensions were the inner dimensions of the channel. The contemplated wavelength was to be one foot with six electrodes per wavelength. This wavelength would require a laminar

flow velocity of 60 feet per second. Although the flow velocity was achievable with the fan used, conditions were turbulent rather than laminar, and the use of compressed air in the exciter did not improve conditions either. The compressed air alone yielded a flow velocity greater than 60 feet per second. The actual wavelengths achieved were much greater than one foot, but the ratio of wavelength to the width dimension permitted the use of the long wavelength limit in the solution to the field equations. Figure 7 shows the entire generator assembly.

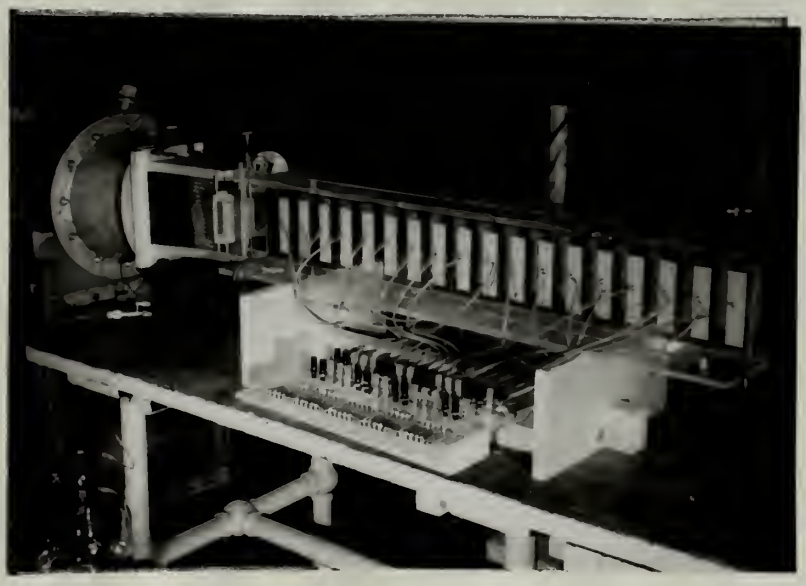

Figure 7: The entire generator assembly. Note the electrodes and load resistor connections.

## RESULTS

The design of the basic generator was centered around practical considerations and the availability of materials. This, however, introduced severe limitations. The flow velocity of the fan was in a region of marked turbulence. The interaction of the nozzle air supply with the fan was such that control of the resultant velocity of the air stream was limited to a samll range. Much higher velocities are necessary to contain the spread of the particle flow, and these higher velocities in turn will more closely approach laminar flow conditions within the channel.

Wetting of the channel proved to be a severe problem also because of its effect on the loss of effective charge. Figures 8 and 9 show the rapid deterioration of the signal in the channel. The combination of turbulence and wetting yielded an erratic current level pattern but the pattern basically repeated itself under all conditions of load. Uniform current levels were finally obtained near the end of the channel where turbulence effects can be considered mollified and the wetting was severe but uniform throughout. However, the output current in this region was drastically reduced.

Another effect noted was the fact that the rate of wetting can be increased by increasing the charging voltage on the exciter. This was to be expected because of the increasing repulsive forces between the

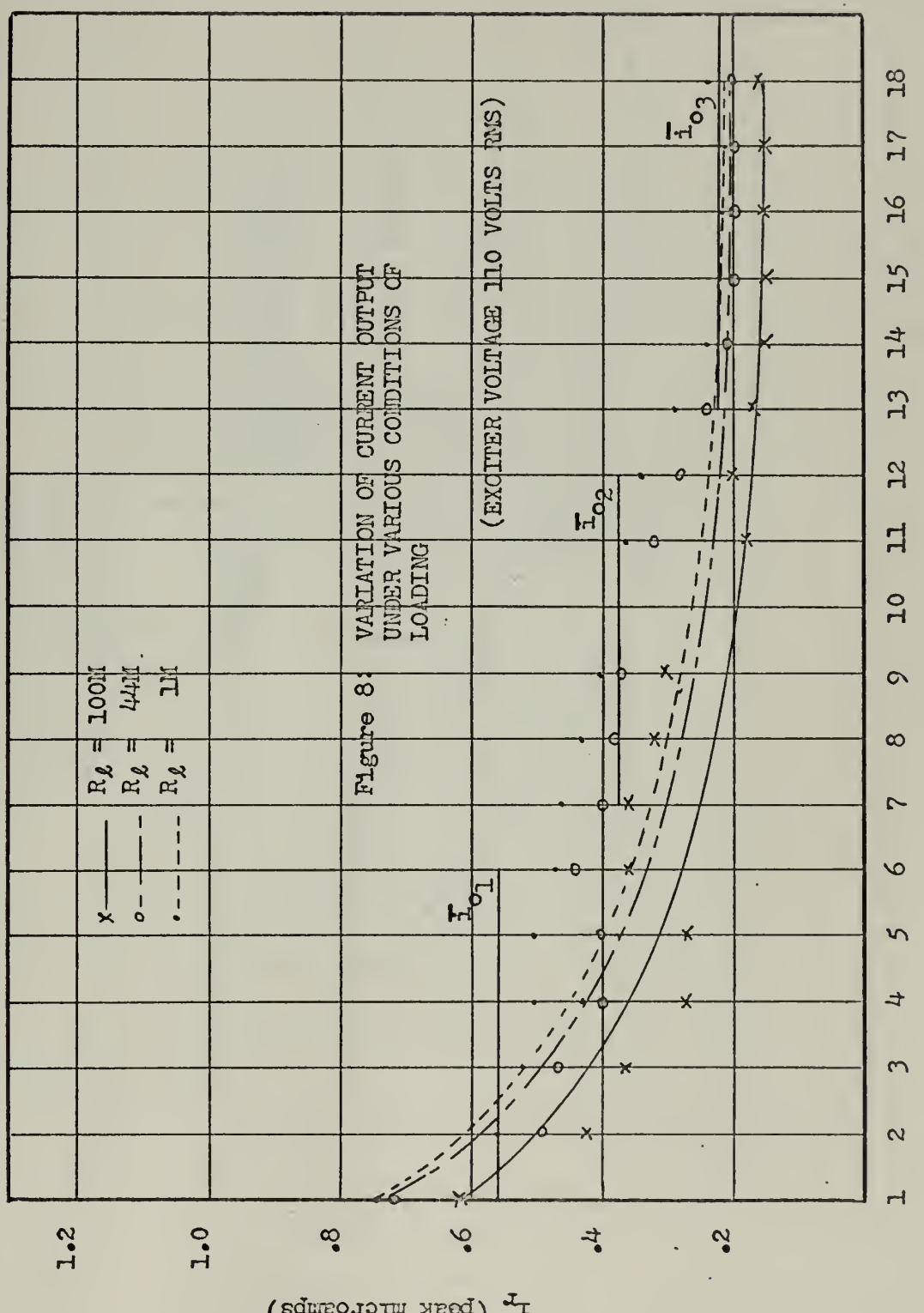
1.2
1.0
.8
.6
.4
.2
$i_r$ (peak microamps)
1 2 3 4 5 6 7 8 9 10 11 12 13 14 15 16 17 18
ELECTRODES
$I_{o1}$
$I_{o2}$
$I_{o3}$
(EXCITER VOLTAGE 110 VOLTS RMS)
VARIATION OF CURRENT OUTPUT
UNDER VARIOUS CONDITIONS OF
LOADING
Figure 8:
x—— $R_\ell$ = 100M
o-- —— $R_\ell$ = 44M
•-- —— $R_\ell$ = 1M

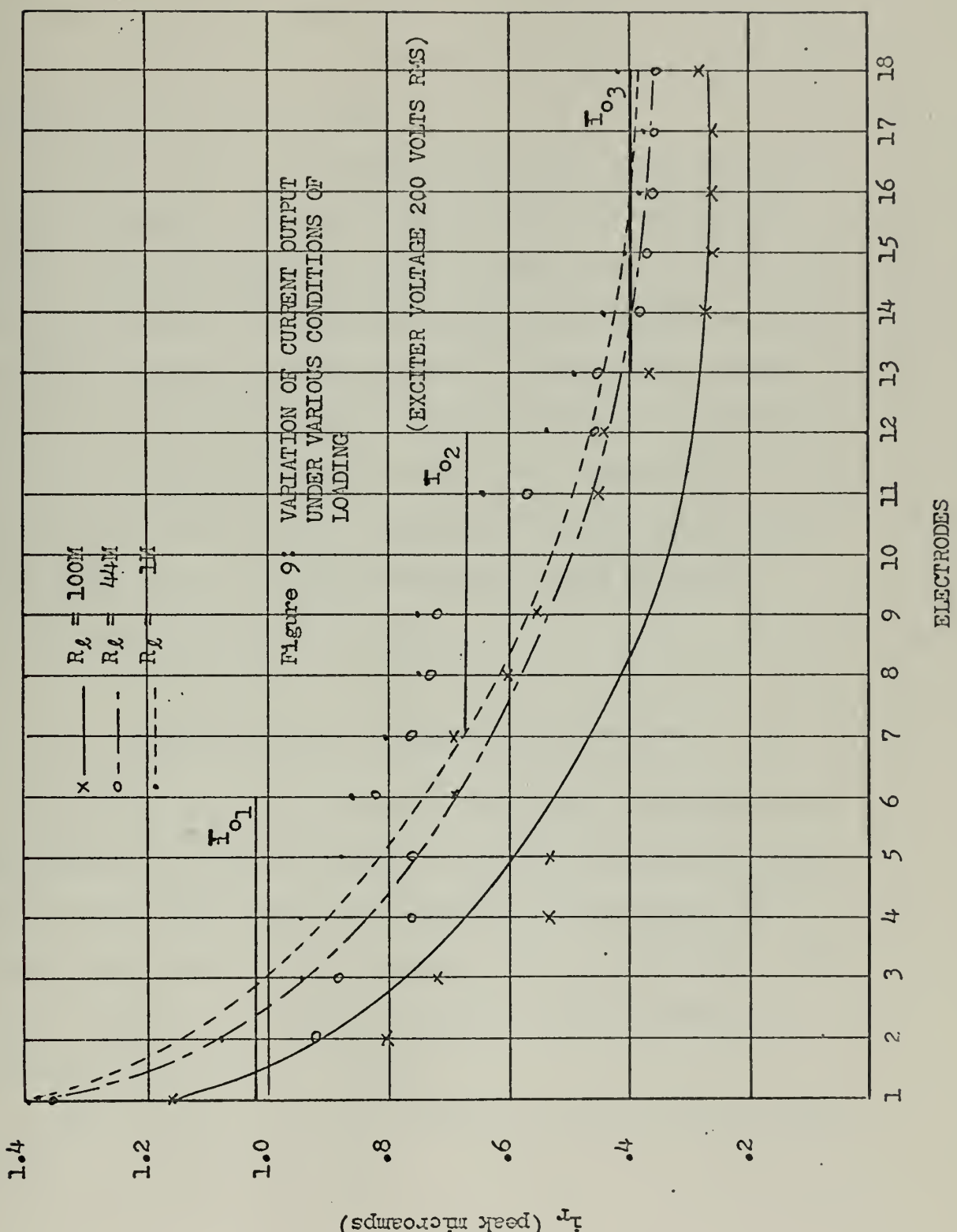


Figure 9: VARIATION OF CURRENT OUTPUT UNDER VARIOUS CONDITIONS OF LOADING (EXCITER VOLTAGE 200 VOLTS R.M.S)

particles. Once wetting had started, it continued until it reached an equilibrium saturation point and little could be done to halt its progress with the present design.

In order to test the validity of the circuit model approach to the entire generator, some adjustment in the theory was necessary because of the variation in the output current levels. To this end the entire generator was modeled as a device containing three bands of current generators with six generators per band. The current generators in each band possess a current $\overline{i_o}$ which is an average of the current levels in each of the three bands. Figures 8 and 9 also show the band level selected. Passive parametersfor the equivalent circuit were chosen from typical electrode loading behavioral characteristics for each band level.

## Equivalent Circuit Modeling of the Generator

The behavior of electrodes under conditions of increased resistive loading are shown in figures 10 and 11. The electrodes shown (2, 9, and 16) were typical of the behavior in each band. The reactance was computed at two charging voltages and averaged. Only a minor discrepancy was noted in each case, and this would be consistent with normal data error.

The manner in which this was done can be ascertained by a quick look at the equivalent circuit.

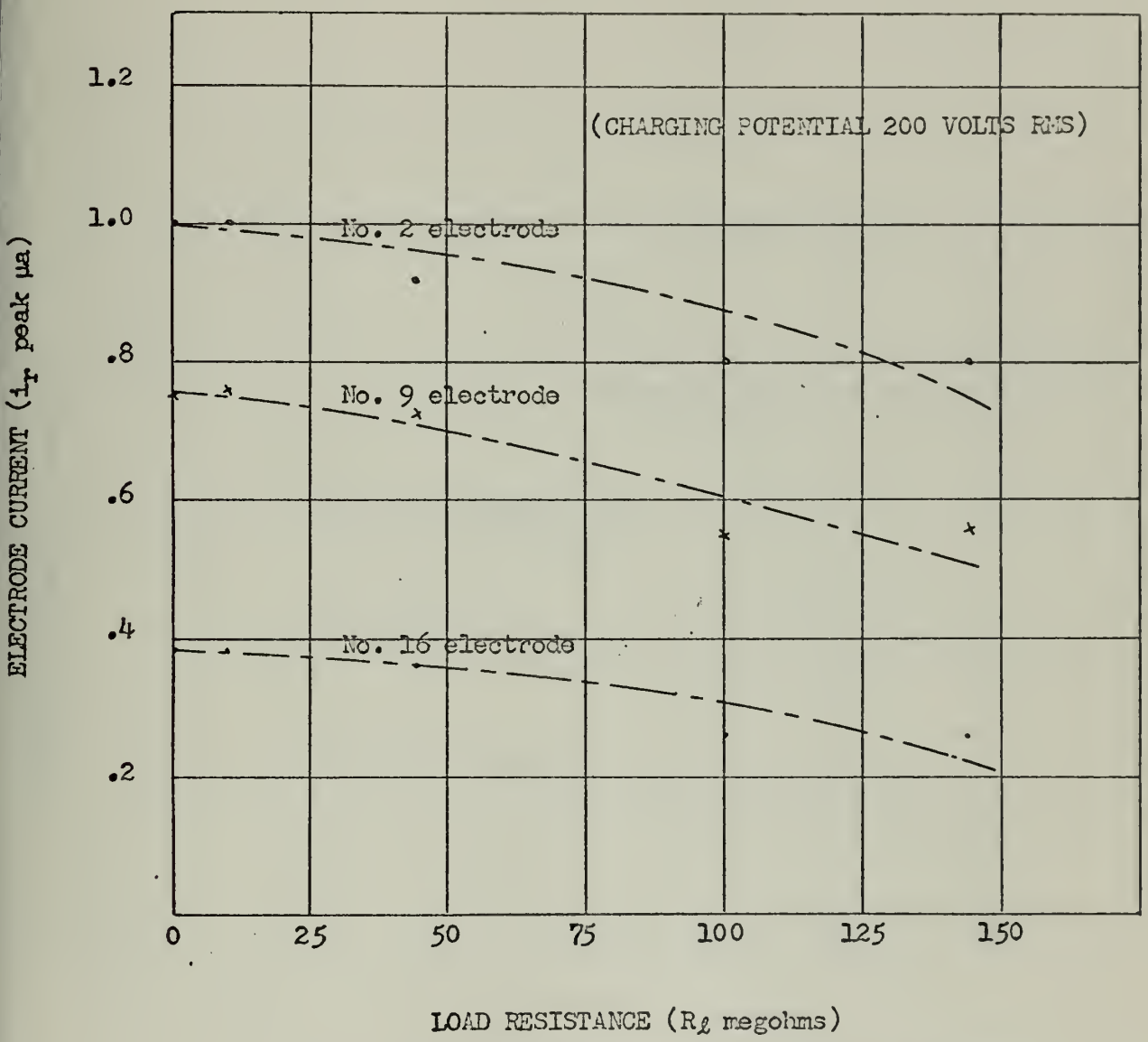


Figure 10: ELECTRODE BEHAVIOR UNDER CONDITIONS OF INCREASING LOAD RESISTANCE

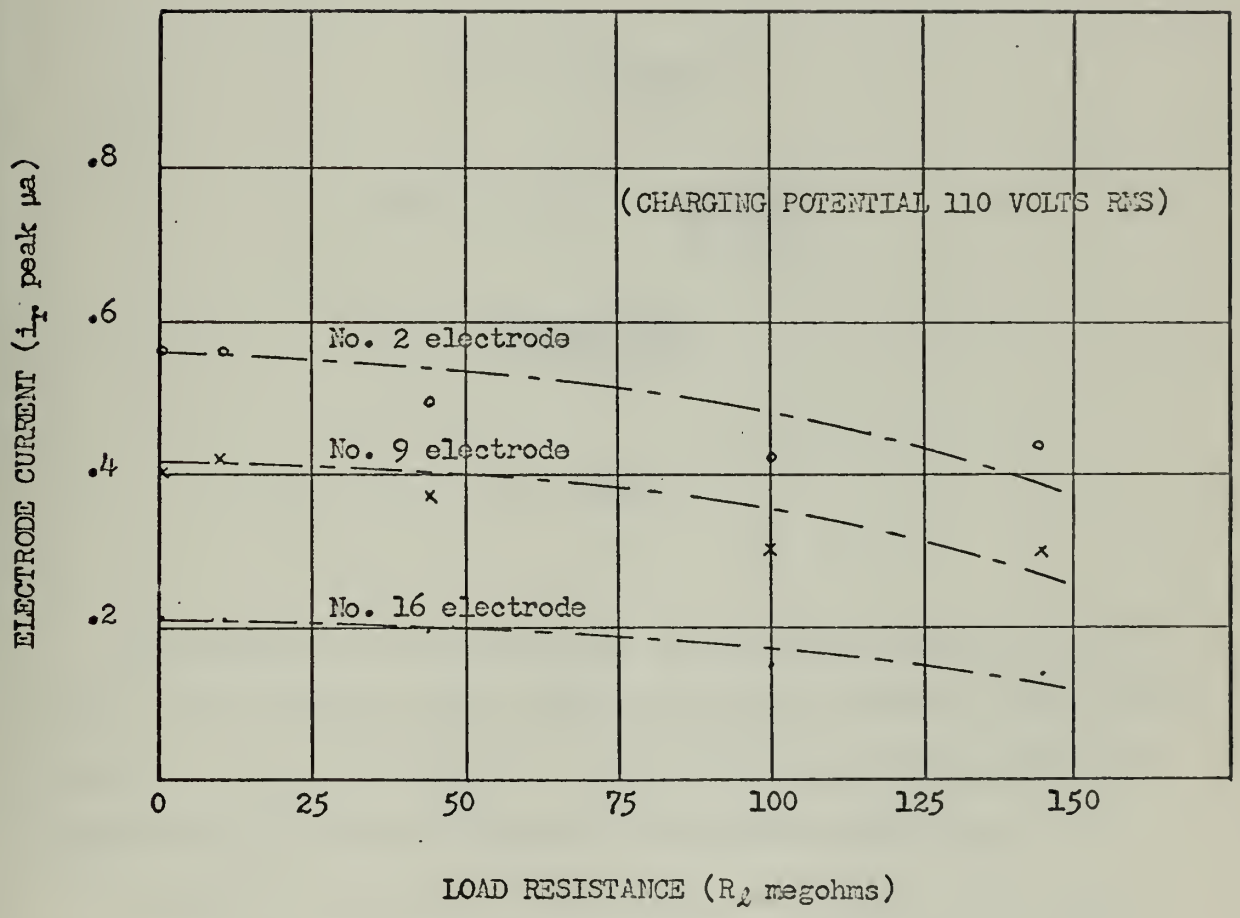


Figure 11: ELECTRODE BEHAVIOR UNDER CONDITIONS OF INCREASING LOAD RESISTANCE

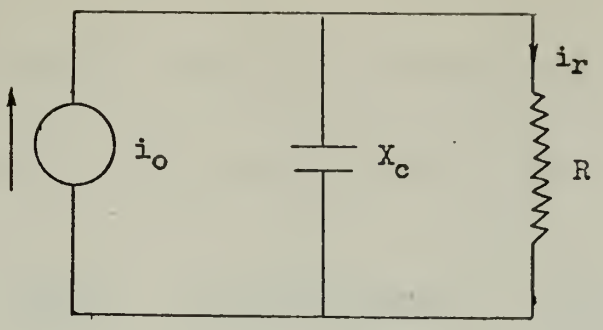


$$i_r = \frac{-j\,Xc\,i_o}{R - j\,Xc}$$

$$i_r^2 = i_r i_r^* = \frac{Xc^2\,i_o^2}{R^2 + Xc^2}$$

$$Xc = \frac{R}{\sqrt{(i_o/i_r)^2 - 1}}$$

$$C = \frac{1}{\omega\,Xc}$$

The current at a load resistance of one megohm effectively represents a short circuit current which would be the current of the current generator or $i_o$. The current at a load resistance of 100 megohms was selected for $i_r$. This was obtained from figures 10 and 11.

In order to correct for current levels an average current based on a square root approximation was used for each band, that is

$$\bar{i}_o = \sqrt{\frac{\sum(i_n)^2}{n}}$$

Six pair of electrodes exist in each current band, hence n = 6.

The results of the calculations are tabulated below:

| Electrode | Xc(MΩ) | C(μμf/electrode) | $\bar{i}_o$ (μa) (110V) | $\bar{i}_o$ (μa) (200V) |
|---|---|---|---|---|
| 2 | 157 | 16.9 | .557 | 1.017 |
| 9 | 130 | 20.4 | .376 | .670 |
| 16 | 124 | 21.5 | .221 | .398 |

In order to test the validity of modeling the generator in this fashion, the power output of the model was computed for several values of load resistance and compared to the experimental values achieved. Figure 12 shows the results of this comparison. A reasonable agreement is achieved so that some validity appears to exist for the derived circuit model.

## Wavelength Measurements

One rather obvious fact not mentioned as yet is the phase delay which occurs in the induced voltage on the electrodes. This is related to the frequency, particle velocity and the distance of the electrode pair from a given reference electrode. Let electrode pair A be the reference electrode, and electrode pair B be another electrode located a distance L downstream from A. The voltages induced in A and B would then be:

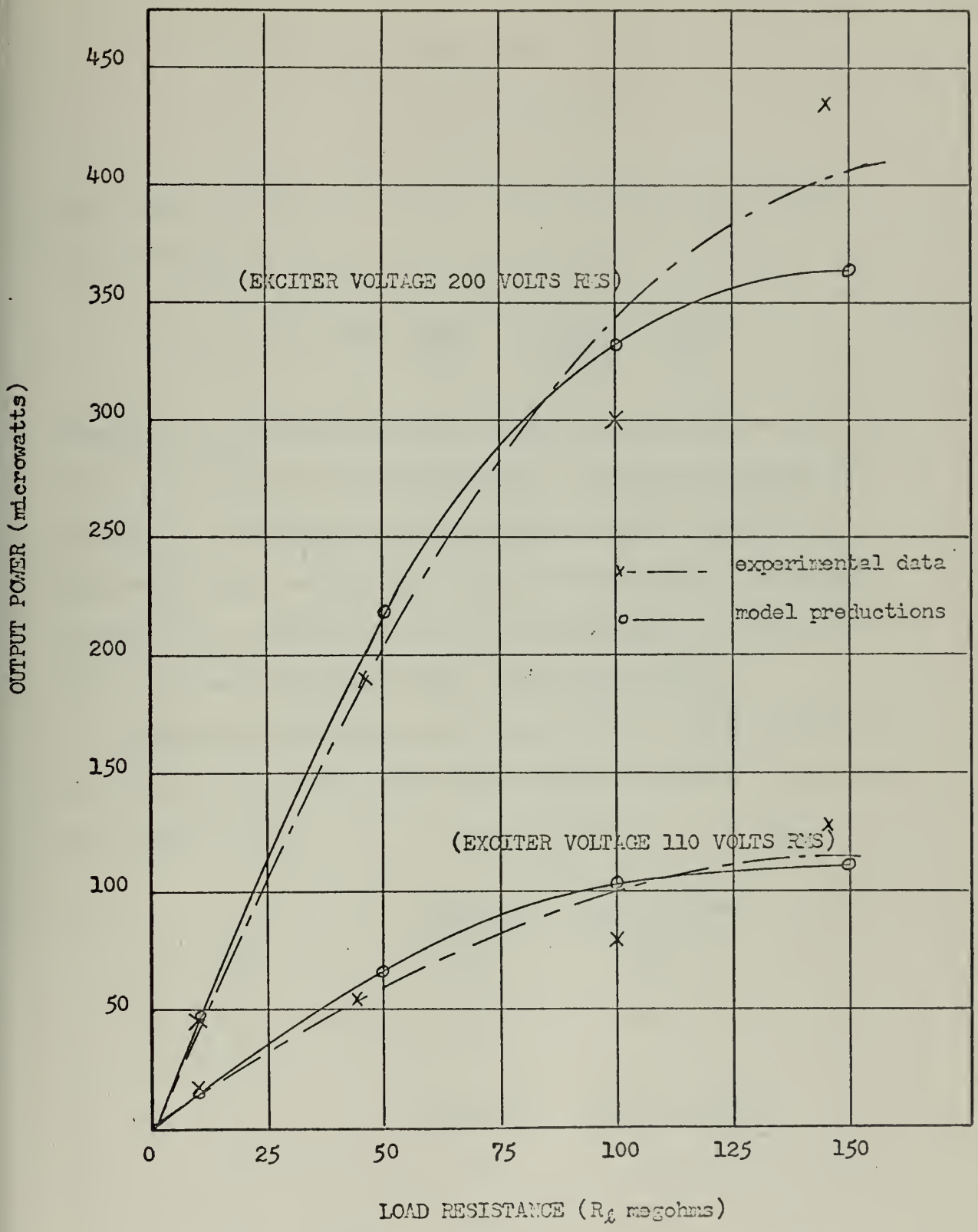


Figure 12: THE VARIATION OF OUTPUT POWER AS A FUNCTION OF LOAD RESISTANCE

$$v_a = \mathrm{Re}\ V_a\, \epsilon^{j\omega t}$$

$$v_b = \mathrm{Re}\ V_b\, \epsilon^{j(\omega t - kL)}$$

Many important relationships can be deduced from the phase shift angle $\theta$ since:

$$\theta = kL = \frac{2\pi L}{\lambda} = \frac{2\pi f L}{v_p} = \frac{\omega L}{v_p} \qquad (5)$$

Therefore, the wavelength and the particle velocity may be measured directly from phase shift considerations. Since the pressure and velocity in the channel were continually changing, the values inferred by these measurements were an average value. The accuracy of phase shift measurements from an oscilloscope is somewhat limited, but significant changes can yield appreciable insight.

Wavelength measurements were taken under two loading conditions at the entrance and exit ends of the electrode chamber. The results are tabulated below:

| | $\lambda_{ent}$(ft) | $v_p$(ft/sec)ent |
|---|---|---|
| $R_\ell = 0$ | 1.403 | 84.2 |
| $R_\ell = 144M$ | 1.333 | 80.0 |

| | $\lambda_{exit}$(ft) | $v_p$(ft/sec)exit |
|---|---|---|
| $R_\ell = 0$ | 1.29 | 77.9 |
| $R_\ell = 144M$ | 1.28 | 73.5 |

In order to check the relative magnitude of these quantities, manometer readings were taken at the beginning and end of the channel to measure the flow velocity. These readings indicated an entrance velocity of 77 feet per second and an exit velocity of 67 feet per second. Complete agreement between the two measurements is out of the question since the manometer is measuring the velocity at a discrete point in a turbulent air flow, while the oscilloscope measurements are based on an averaging process. The agreement between the velocity figures is satisfactory, however.

The changes in wavelength do demonstrate the increasing interaction of the particles and the induced voltages as the load resistance is increased. Whether or not this is directly related to the slip indicated by the negative stress tensor of Appendix A I is questionable at this point, but the results do demonstrate that the change in wavelength is greater in the entrance portion of the channel where the effective charge is proportionately greater.

## CONCLUSIONS AND RECOMMENDATIONS

The basic premise of the thesis was to demonstrate the qualitative aspects of an EHD traveling-wave synchronous generator. This has been accomplished. The proposed circuit model does seem to predict the generator behavior within tolerable limits. In addition, the phase shift measurements do demonstrate the interaction of the charged particles with the induced voltages.

The generator has also clearly shown the conflicting problems which are inherent in the design of such a system. Several of these have been ignored in the discussion so far, but are mentioned in the following list of salient considerations for perfecting the design:

1. The flow velocity used is in a region of a turbulent Reynolds number. Much higher velocities will be necessary to counteract the turbulence effect.

2. The inherent spreading characteristic of a nozzle causes the electrode channel to wet. This reduces the effective charge present in the channel. Higher flow velocities should help to reduce this effect, but nozzle devices are necessary for providing the copious quantities of charged particles needed.

3. Data from the exciter indicates that the charge deposited on the water droplets is directly proportional to the charging potential in the charging potential regions tested. Increasing the exciter voltage increases the explosion tendency

of the particle beam and hence promotes wetting.

4. External capacitive effects are far greater than anticipated from the predicted values. The capacitance is an order of magnitude greater than the preliminary estimates suggested. It is this capacitive effect which leads to the early loading of the generator. Much of this capacitive effect may be in the wiring leads, and can be eliminated easily.

5. The generator is capable of operating advantageously with electrodes connected in parallel if laminar flow conditions can be approached and the capacitive effects reduced.

6. The feasibility of operating the generator self excited seems very plausible as design improvements are incorporated into the basic device.

7. The dimensions of the electrodes need to be optimized.

8. Particle size and mobility need to be studied in much greater detail.

The problems which must be overcome in order to perfect this type of system are quite numerous and will entail considerable time and genius but certainly many improvements are capable of being incorporated into the basic design.

The relative merits of this prototype should be studied in comparison to recent developments on a DC EHD ballistic generator. Maximum

currents achieved on this device have approached 260 μ a with a charging potential of 50 KV. The ratio of output current to charging potential in the DC device is $5.2 \times 10^{-9}$. The AC device produces a ratio of peak current to peak charging potential of $5.02 \times 10^{-9}$. Paralleling of electrodes in the AC device can improve staging outputs far beyond this level. Grids must be employed in order to stage the DC output.

The prototype has demonstrated that the future does hold some promise for AC EHD generators. The problems in perfecting the design are recognizable which is the first step in achieving a practical engineering system.

# APPENDIX A I

## DERIVATION OF THE EXPRESSION FOR DEVELOPED EHD POWER

Derivation of the Expression for Developed EHD Power

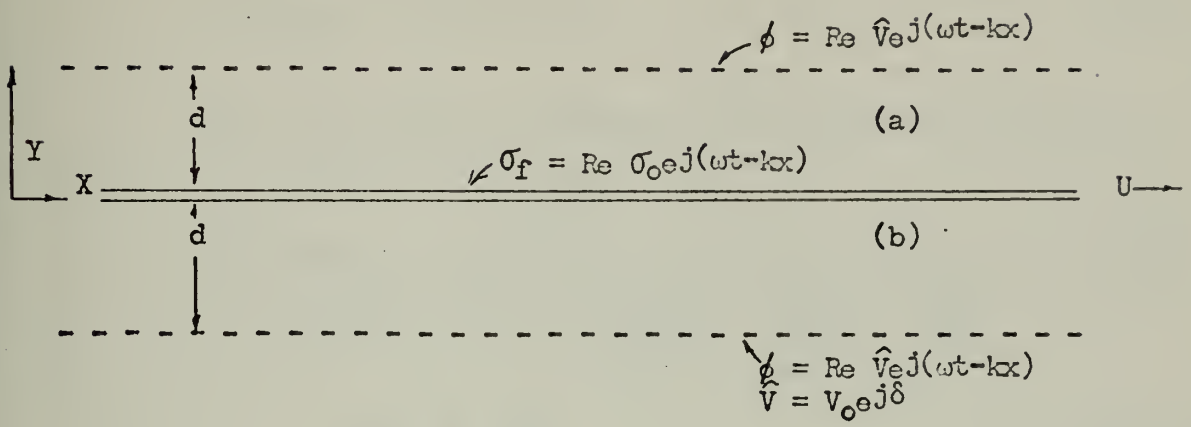


Figure A-1-1. Top view of an AC EHD synchronous generator

In regions (a) and (b) Maxwell's equations yield the following:

$$\nabla \times \vec{E} = 0. \qquad \text{(A-1-1)}$$

Therefore, $\vec{E} = -\nabla \hat{\phi}$ and (A 1-2)

$$\nabla \cdot \epsilon_o \vec{E} = 0 \qquad \text{(A-1-3)}$$

Equations (A-1-2) and (A-1-3) imply that LaPlace's equation must hold in these regions. That is

$$\nabla^2 \hat{\phi} = 0. \qquad \text{(A-1-4)}$$

Finally, because of the traveling wave dependence $\hat{\phi}$ must be of the form $\hat{\phi} = \text{Re } \hat{\phi}(y) \epsilon^{j(\omega t-kx)}$. The geometry of the configuration in view of LaPlace's equation generates the form of the solution, which is:

$$\hat{\phi}_a = \hat{A} \cosh ky + \hat{B} \sinh ky \qquad \text{(A-1-5)}$$

$$\hat{\phi}_b = \hat{C} \cosh ky + \hat{D} \sinh ky \qquad \text{(A-1-6)}$$

Sufficient boundary conditions exist to evaluate all of the constants. They are as follows:

(1) At the electrode boundary the potential is $\hat{V}$.

$$\hat{\phi}_a(d) = \hat{V} \qquad \hat{\phi}_b(-d) = \hat{V}$$

$$\hat{A} \cosh kd + \hat{B} \sinh kd = \hat{V} \tag{A-1-7}$$

$$\hat{C} \cosh kd - \hat{D} \sinh kd = \hat{V} \tag{A-1-8}$$

(2) The tangential component of the electric field must be continuous at $y = 0$.

$$\hat{A} = \hat{C} \tag{A-1-9}$$

(3) The normal component of the electric field at $y = 0$ must equal $\frac{\sigma_o}{\epsilon_o}$, that is $- \frac{\partial \hat{\phi}_a(o)}{\partial y} + \frac{\partial \hat{\phi}_b(o)}{\partial y} = \frac{\sigma_o}{\epsilon_o}$

$$- k\hat{B} + k\hat{D} = \frac{\sigma_o}{\epsilon_o} \tag{A-1-10}$$

The boundary conditions may be summarized as follows, using matrix notation.

$$\begin{bmatrix} \cosh kd & 0 & \sinh kd & 0 \\ 0 & \cosh kd & 0 & -\sinh kd \\ 1 & -1 & 0 & 0 \\ 0 & 0 & -1 & 1 \end{bmatrix} \cdot \begin{bmatrix} \hat{A} \\ \hat{C} \\ \hat{B} \\ \hat{D} \end{bmatrix} = \begin{bmatrix} \hat{V} \\ \hat{V} \\ 0 \\ \sigma_o / k\epsilon_o \end{bmatrix}$$

In order to determine the electrohydrodynamic power which is available for extraction as electrical power, it is necessary to determine the time average retarding stress tensor acting on the stream of charged particles. The total stress tensor

$T_x$ = force per unit area on the stream.

$$T_x = (T_{xy}^a - T_{xy}^b) \tag{A-1-11}$$

$$\begin{array}{c} T_{xy}^a \\ \hline\hline \\ T_{xy}^b \end{array}$$

Therefore, $\tau_x = \epsilon_o (\hat{E}_x^a \hat{E}_y^a - \hat{E}_x^b \hat{E}_y^b)\Big|_{(y=0)}$

$$= \epsilon_o \hat{E}_x^a (\hat{E}_y^a - \hat{E}_y^b) \qquad (y=0) \qquad \text{(A-1-12)}$$

The time average value of $\tau_x$ may be expressed in the following fashion:

$$\langle \tau_x \rangle = 1/2\epsilon_o \, \mathrm{Re}\, \hat{E}_x^{a*} (\hat{E}_y^a - \hat{E}_y^b)\Big|_{(y=0)} \qquad \text{(A-1-13)}$$

Evaluation of the desired quantities reduces the expression to the constants of the field equations.

$$\hat{E}_x^a = - jk \hat{\phi}_a \qquad \hat{E}_x^a (y=0) = - jk\hat{A} \qquad \text{(A-1-14)}$$

$$\hat{E}_y = \frac{\partial \hat{\phi}}{\partial y} \qquad \hat{E}_y^a (y=0) = - \hat{B} k$$

$$\hat{E}_y^b (y=0) = - \hat{D} k \qquad \text{(A-1-15)}$$

$$\langle \tau_x \rangle = 1/2 \, \epsilon_o \, \mathrm{Re} jk^2 \hat{A}^* (\hat{B} - \hat{D}) \qquad \text{(A-1-16)}$$

Symmetry requires that $\hat{B} = - \hat{D}$.

$$\langle \tau_x \rangle = \epsilon_o \mathrm{Re} jk^2 \hat{A}^* \hat{B} \qquad \text{(A-1-17)}$$

Evaluation of the constants from the matrix shows that,

$$\hat{A} = \frac{\hat{V}}{\cosh kd} + \frac{\sigma_o}{2k\epsilon_o} \tanh kd \qquad \text{(A-1-18)}$$

$$\hat{B} = \frac{-\sigma_o}{2k\epsilon_o} \qquad \text{(A-1-19)}$$

Substitution of equation (A-1-18) and (A-1-19) into equation (A-1-17) yields the desired result.

$$\langle T_x \rangle = - \frac{Re jk V^* \sigma_o}{2 \cosh kd} = - \frac{k V_o \sigma_o}{2 \cosh kd} \sin \delta \qquad \text{(A-1-20)}$$

The time average electrohydrodynamic developed power capable of being extracted from the stream is,

$$P_d = | \langle T_x \rangle | \, AU \qquad \text{(A-1-21)}$$

where A is the total lateral area of the stream. If the chamber has a length L, and an effective electrode or stream height a, then the power may be expressed in the following forms:

$$P_d = \frac{k V_o \sigma_o}{2 \cosh kd} L \, a \, U \sin \delta \qquad \text{(A-1-22)}$$

$$= \frac{2\pi V_o \sigma_o}{2\lambda \cosh kd} L \, a \, U \sin \delta \qquad \text{(A-1-23)}$$

$$= \frac{\omega V_o \sigma_o}{2 \cosh kd} L \, a \sin \delta \qquad \text{(A-1-24)}$$

where $\omega$ is the synchronous frequency of the system.

Since discrete electrodes are being used, the expression for power developed should be corrected to reflect the fact that the interaction occurs only when the charged particles are under the influence of the electrodes. If an area efficiency is defined, then a proper correction factor may be applied.

$$\eta_a = \frac{\text{A electrodes}}{\text{A lateral}} \qquad \text{(A-1-25)}$$

$$\eta_a = \frac{\text{Number of pairs of electrodes x electrode area}}{\text{A lateral}}$$

$$= \frac{Nac}{aL} = \frac{Nc}{L} \qquad \text{(A-1-26)}$$

where N = number of pairs of electrodes

c = electrode width

$$P_d' = P_d \eta_a$$

$$= \frac{Nac}{\cosh kd} \omega V_o \sigma_o \sin \delta$$

$$= K_e' \omega V_o \sigma_o \sin \delta \qquad \text{(A-1-27)}$$

# APPENDIX A II

## DERIVATION OF THE OUTPUT POWER DELIVERED TO A CONTINUOUS RESISTIVE LOADING

Derivation of the Output Power Delivered to a

Continuous Resistive Loading

The system is now depicted as shown in figure A-2-1. The segmented

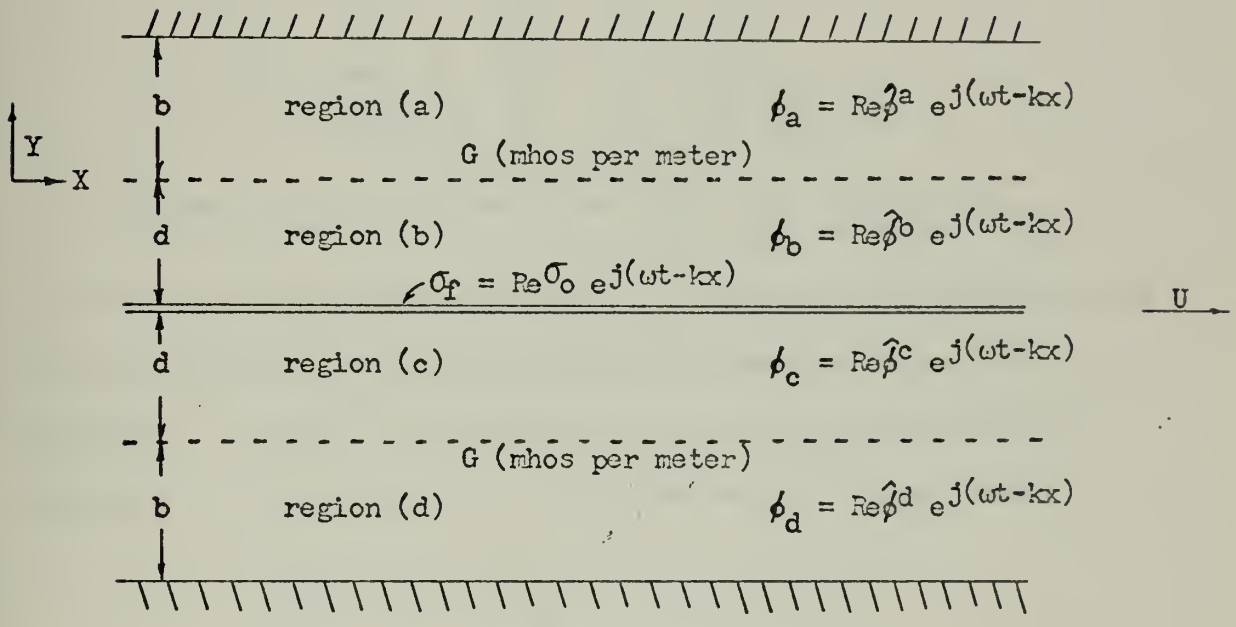


Figure A-2-1. Top View of a Continuously Loaded AC EHD

Synchronous Generator

electrodes are distributed along the X axis and at Y = -2d. The generator is again symmetric about the stream of charged particles, so that the solutions to the field equations for the upper regions (a) and (b) are equally applicable to the lower regions also. The resistive loading connects the electrodes to ground planes which are located at Y = b, and Y = - (b+d). The electrodes have a height "a" which extends into

the paper.

The end view of the generator is as shown in figure A-2-2. The

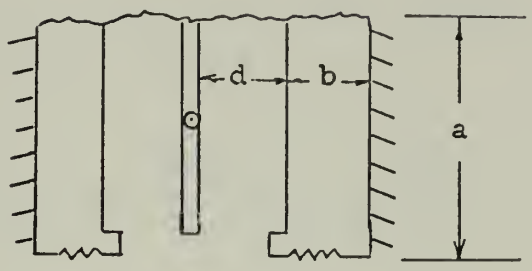


Figure A-2-2. End View of the Synchronous Generator.

resistive load may be assumed to have a conductance of G mhos per meter in the X direction. The end view again demonstrates the symmetry of the generator. In view of the symmetry involved, the potential may be assumed to have a distribution of the form shown in figure A-2-3.

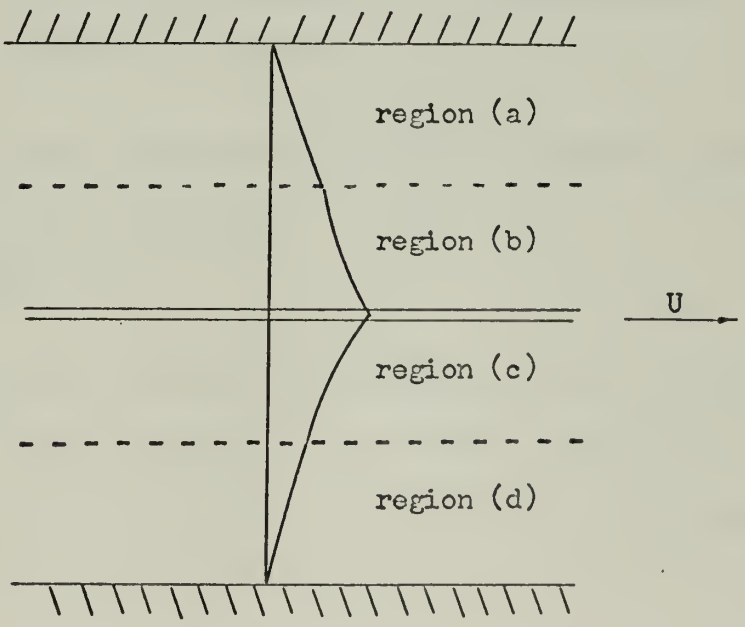


Figure A-2-3. Potential Distribution of a Continuously Resistive Load.

In order to evaluate the entire solution, it is again necessary to consider the boundary conditions. These are:

1. The normal component of the electric field at y = -d must be equal to $\sigma_o/\epsilon_o$. That is

$$\left.\frac{-\partial\hat{\phi}^b}{\partial y}\right|_{(y=-d)} + \left.\frac{\partial\hat{\phi}^c}{\partial y}\right|_{(y=-d)} = \frac{\sigma_o}{\epsilon_o} \qquad \text{(A-2-1)}$$

In addition symmetry requires $\left.\frac{\partial\hat{\phi}^b}{\partial y}\right|_{(y=-d)} = \left.\frac{-\partial\hat{\phi}^c}{\partial y}\right|_{(y=-d)}$,

so that equation (A-2-1) reduces to

$$-2\,\frac{\partial\hat{\phi}^b}{\partial y}(-d) = \frac{\sigma_o}{\epsilon_o} \quad . \qquad \text{(A-2-2)}$$

2. The potentials must be continuous at the electrodes.

$$\hat{\phi}^a(0) - \hat{\phi}^b(0) = 0 \qquad \text{(A-2-3)}$$

3. At the ground planes, the potential is defined as the point of zero potential.

$$\hat{\phi}^{a(b)} = 0 \qquad \text{(A-2-4)}$$

4. Conservation of charge on the electrode surface provides the final boundary condition. If we define the charge per unit length in the X direction as $q_s$, then the normal components of the electric field require that

$$q_s = -a\epsilon_o \left[ \left. \frac{\partial \hat{\phi}^a}{\partial y} \right|_{(y=0)} \quad \left. \frac{-\partial \hat{\phi}^b}{\partial y} \right|_{(y=0)} \right] \tag{A-2-5}$$

Considering the conductance per unit length in the X direction across an electrode of height a, conservation of charge states that

$$\frac{-\partial q_s}{\partial t} = \hat{\phi}^a(0)\, G. \tag{A-2-6}$$

Substitution of equation (A-2-5) into (A-2-6) yields the final result.

$$j\,\omega\, a\, \epsilon_o \left[ \frac{\partial \hat{\phi}^a}{\partial y}(0) - \frac{\partial \hat{\phi}^b}{\partial y}(0) \right] = G\, \hat{\phi}^a(0) \tag{A-2-7}$$

The singularities in the charge distribution at the boundaries require that the solutions be at least piecewise continuous. The traveling wave dependence of $\sigma_f$ requires that the solution be of the form $\phi = \mathrm{Re}\, \hat{\phi}(y)\, e^{j(\omega t - kx)}$. In addition, La Place's equation holds in regions (a) and (b), hence the geometry suggests the form of the solution.

$$\hat{\phi}^a = \hat{A} \sinh ky + \hat{B} \cosh ky \tag{A-2-8}$$

$$\hat{\phi}^b = \hat{C} \sinh ky + \hat{F} \cosh ky \tag{A-2-9}$$

The boundary conditions may now be rewritten utilizing the known form of the solution. Equation (A-2-2) requires that

$$2\,\epsilon_o k \left[ \hat{C} \cosh kd - \hat{F} \sinh kd \right] = -\sigma_o \tag{A-2-10}$$

Equation (A-2-3) requires that

$$\hat{B} - \hat{F} = 0 \qquad \text{(A-2-11)}$$

while equation (A-2-4) states that

$$\hat{A} \sinh kb + \hat{B} \cosh kb = 0. \qquad \text{(A-2-12)}$$

Finally, the fourth equation comes from (A-2-7) which states that

$$j \omega a \epsilon_o k[\hat{A} - \hat{C}] = G \hat{B}. \qquad \text{(A-2-13)}$$

These results may be summarized in matrix form as follows:

$$\begin{bmatrix} 0 & 0 & \cosh kd & -\sinh kd \\ 0 & 1 & 0 & -1 \\ \sinh kb & \cosh kb & 0 & 0 \\ 1 & jG/\omega a\epsilon_o k & -1 & 0 \end{bmatrix} \cdot \begin{bmatrix} \hat{A} \\ \hat{B} \\ \hat{C} \\ \hat{F} \end{bmatrix} = \begin{bmatrix} -\sigma_o/2\epsilon_o k \\ 0 \\ 0 \\ 0 \end{bmatrix}$$

In order to determine the power output per unit length, it is necessary to consider a slight digression at this point. The power delivered to the resistive load is $P_1$.

$$P_1 = G \hat{\phi}^a(0)^2 \qquad \text{(A-2-14)}$$

On a time average basis this reduces to

$$\langle P_1 \rangle = \frac{G}{2} \hat{\phi}^a(0).\hat{\phi}^{a*}(0) = \frac{G}{2} \hat{B}.\hat{B}^* \qquad \text{(A-2-15)}$$

Thus the matrix need only be solved for $\hat{B}$ to determine the output power.

$$\hat{B} = \frac{\frac{\sigma_o \sinh kb}{2\epsilon_o k}}{\cosh k(b+d) - \frac{jG}{\omega a \epsilon_o k} \sinh kb \cosh kd} \qquad \text{(A-2-16)}$$

Thus, the time average power delivered to the load per unit length is as follows:

$$\langle P_l \rangle = \frac{\frac{G}{2}\left[\frac{\sigma_o \sinh kb}{2\epsilon_o k}\right]^2}{\cosh^2 k(b+d) + \left(\frac{G}{\omega a \epsilon_o k}\right)^2 \sinh^2 kb \cosh^2 kd} \qquad \text{(A-2-17)}$$

A brief examination $\langle P_l \rangle$ shows that an optimum value of G exists for maximum power transfer,

$$G_{opt} = \frac{\omega a \epsilon_o k \left( \cosh k(b+d) \right)}{\sinh kb \cosh kd} \cdot \qquad \text{(A-2-18)}$$

Therefore, the maximum power transfer may be determined.

$$\langle P_l \rangle_{max} = \frac{G_{opt}}{4} \frac{\left[\frac{\sigma_o \sinh kb}{2\epsilon_o k}\right]^2}{\cosh^2 k(b+d)} \qquad \text{(A-2-19)}$$

Although the equations appear to be somewhat complicated at this point, it is worthy to consider the long wavelength limit of their form, i. e. kb and kd << 1. This reduces the complexity of the mathe-

matics considerably. Equation (A-2-17), (A-2-18), and (A-2-19) reduce to:

$$\langle P_1 \rangle = \frac{G\,\sigma_o^2\,\omega^2\,a^2\,b^2}{8\left[\omega^2\,a^2\,\epsilon_o^2 + G^2\,b^2\right]} \qquad \text{(A-2-20)}$$

$$G_{opt} = \frac{\omega\,a\,\epsilon_o}{b} \qquad \text{(A-2-21)}$$

$$\langle P_1 \rangle_{max} = \frac{\sigma_o^2\,\omega\,a\,b}{16\,\epsilon_o} \qquad \text{(A-2-22)}$$

The total maximum power output of a chamber of length L will be equal to

$$\langle P_1 \rangle_{max} = \frac{\sigma_o^2\,\omega\,a\,b\,L}{16\,\epsilon_o} \qquad \text{(A-2-23)}$$

However, this expression should also be corrected for the area efficiency mentioned in Appendix A I.

$$\langle P_1 \rangle'_{max} = \langle P_1 \rangle_{max}\,\eta_a = \frac{\sigma_o^2\,\omega\,a\,b\,c\,N}{16\,\epsilon_o} \qquad \text{(A-2-24)}$$

$$\langle P_1 \rangle'_{max} = K\,\sigma_o^2\,\omega \qquad \text{(A-2-25)}$$

# APPENDIX A III

## DETERMINATION OF AN EQUIVALENT CIRCUIT MODEL

Determination of an Equivalent Circuit Model

Appendix A II developed the expression for the time average power delivered to the load per unit length. Manipulation of this power expression will yield correct dimensional quantities for infering an equivalent circuit for a per unit length. Equation (A-2-17) will serve as a basis for this development.

$$\langle P_1 \rangle = \frac{\frac{G}{2}\left[\frac{\sigma_o \sinh kb}{2\epsilon_o k}\right]^2}{\cosh^2 k(b+d) + \left(\frac{G}{\omega a \epsilon_o k}\right)^2 \sinh^2 kb \cosh^2 kd}$$

Considering the long wavelength limit, the equation reduces to the following:

$$\langle P_1 \rangle = \frac{\frac{G}{2}\left[\frac{\sigma_o b}{2\epsilon_o}\right]^2}{1 + \left(\frac{G b}{\omega a \epsilon_o}\right)^2} \quad . \qquad \text{(A-3-1)}$$

Multiplying the numerator by $\left(\frac{\omega a}{\omega a}\right)^2$ and noting that $G = 1/R$ where R is the resistance per unit length in the X direction equation (A-3-1) may be manipulated into the desired form.

$$\langle P_1 \rangle = \frac{\frac{1}{2}\left[\frac{\sigma_o \omega a}{2}\right]^2 \left[\frac{b}{\omega a \epsilon_o}\right]^2 \frac{1}{R}}{\frac{1}{R^2}\left[R^2 + \left(\frac{b}{\omega \epsilon_o a}\right)^2\right]}$$

$$\langle P_1 \rangle = \frac{\frac{1}{2}\left[\frac{\sigma_{o\omega a}}{2}\right]^2 \left[\frac{1}{\omega \epsilon_o (a/b)}\right]^2 R}{R^2 + \left[\frac{1}{\omega \epsilon_o (a/b)}\right]^2} \qquad \text{(A-3-2)}$$

The choice of an appropriate equivalent circuit is governed by the principle of duality. The circuit model for the basic AC synchronous generator utilizing magnetic fields is a voltage source in series with a synchronous inductive reactance and a load resistance. It appears reasonable that an appropriate circuit model for the EHD generator utilizing electric fields would be a dual arrangement employing a current source in parallel with a capacitive synchronous susceptance and a load conductance. To this end, consider the following circuit configuration and the expression for the power

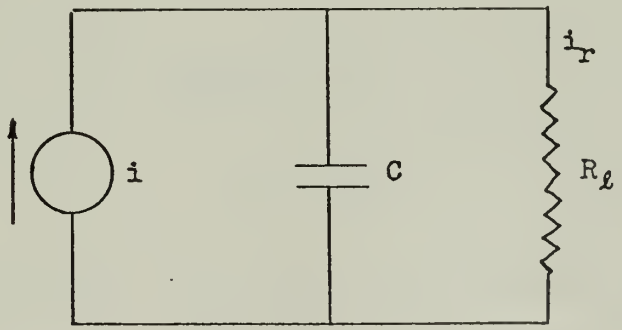


delivered to the load resistance.

$$\langle P_l \rangle = \frac{1}{2} (i_r \, i_r^*) \, R_\ell \qquad \text{(A-3-3)}$$

$$i_r = \frac{i \quad \frac{-j}{\omega C}}{R_\ell - \frac{j}{\omega C}} \qquad \text{(A-3-4)}$$

$$\langle P_l \rangle = \frac{\frac{1}{2} i^2 \left(\frac{1}{\omega C}\right)^2 R_\ell}{R_\ell^2 + \left(\frac{1}{\omega C}\right)^2} \qquad \text{(A-3-5)}$$

By comparing equation (A-3-5) with (A-3-2), the equivalence of terms can be easily recognized. The analogy can be defined as follows:

$$\frac{\sigma_o \, \omega \, a}{2} \doteq i$$

$$\epsilon_o (a/b) \doteq C \qquad \text{(A-3-6)}$$

$$R \doteq R_\ell$$

A comparison of the units of the terms defined in equation (A-3-6) shows that $\frac{\sigma_o \, \omega \, a}{2}$ has the dimensions of amperes per unit length, while $\frac{1}{\omega \, \epsilon_o (a/b)}$ and R have the dimension of ohms per unit length. Therefore, the equivalent circuit defining the time average power delivered to a load resistance on a per unit length basis is depicted on the next page.

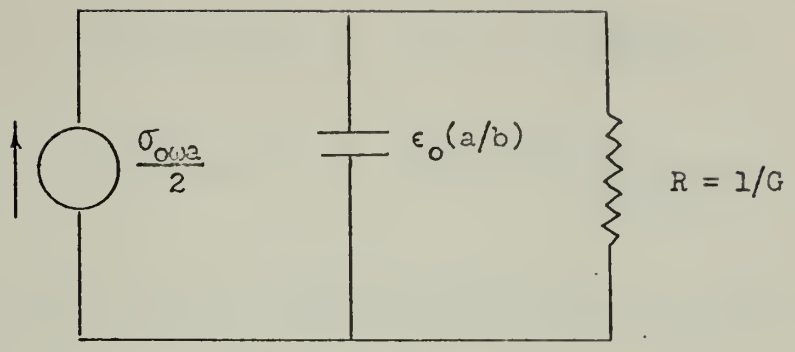


Maximum power transfer in this model will occur when the admittances are equal which is equivalent to an impedance matching condition. That is

$$R \omega C = 1 . \qquad \text{(A-3-7)}$$

This is equivalent to equation (A-2-21) which states that

$$G_{opt} = \epsilon_o \omega(a/b) = \omega C .$$

In order to obtain some feeling for the order of magnitude involved, consider the condition where $a \approx b$, at a frequency of 60 cps.

$$G_{opt} = \epsilon_o \omega = 2\pi \times 60 \times \frac{1}{36 \pi \times 10^9}$$

$$G_{opt} = 3.33 \times 10^{-9} \text{ mhos per meter.}$$

The standard electrode spacing utilized in the generator was one inch, therefore:

$$G_{opt/electrode} = 8.5 \times 10^{-11} \frac{\text{mhos}}{\text{electrode}}$$

$$R_{opt/electrode} = 1.18 \times 10^{10} \frac{\text{ohm}}{\text{electrode}}$$

In addition, the circuit requires that maximum time average power delivered per unit length be equal to

$$\langle P_l \rangle_{max} = \frac{\sigma_o^2 \omega a b}{16 \epsilon_o}$$

which is identical to the maximum power requirements of equation (A-2-22).

# APPENDIX B

# BIBLIOGRAPHY

# BIBLIOGRAPHY

(1) Lawson, M. O., Von Ohain, H., Wattendorf, F., "Performance Potentialities of Direct Energy Conversion Processes between Electrostatic and Fluid Dynamic Energy". ARL 178, Office of Aerospace Research, U.S. Air Force (Dec. 1961)

(2) Lawson, M.O., "Performance Characteristics of Electro Fluid Dynamic Energy Conversion Process Employing Viscous Coupling" ARL 64-74, Office of Aerospace Research, U. S. Air Force (Oct. 1964)

(3) Hasinger, S., "Performance Characteristics of Electro-Ballistic Generators" ARL 64-75, Office of Aerospace Research, U. S Air Force (Oct. 1964)

(4) Fitzgerald, A. E., and Kingsley, C., "Electric Machinery", Second Edition, McGraw Hill, 1961.

(5) Hildebrand, F. B., "Advanced Calculus for Application" Prentice-Hall, 1962.

(6) Fano, R. M., Chu, L. J., Adler, R., "Electromagnetic Fields, Energy, and Forces", John Wiley and Sons, 1960.

(7) Herold, L. "Traveling Wave Charged Particle Generation" SM thesis in preparation, Massachusetts Institute of Technology (1967)